

A study of non-linear Langevin dynamics under non-Gaussian noise with quartic cumulant

Chandan Jana*

*Mandelstam Institute for Theoretical Physics,
Witwatersrand University, Johannesburg, South Africa.*

and

International Centre for Theoretical Sciences, Hesaraghatta, Bangalore, India.

(Dated: June 28, 2022)

We consider a non-linear Langevin equation in presence of non-Gaussian noise with a quartic cumulant. The Langevin description has an equivalent path integral description. We show that the parameters in these two descriptions are related by a renormalisation flow, where the path integral parameters are the renormalised ones. We compute both numerically and analytically the velocity two point function and show that it saturates to the bath temperature even in presence of non-linearity. We also find the velocity four point function numerically and show that it saturates to the analytically evaluated thermal velocity four point function when the non-linear FDR [1] is satisfied. When the non-linear FDR, which is a manifestation of time reversality of thermal bath, is violated then the system does not seem to thermalise. Rather, its velocity four point function settles to a steady state.

CONTENTS

I. Introduction	1
II. Renormalisation of parameters in the discretised problem	2
III. Preparation of noise and particle correlation functions	4
A. Preparation of noise	4
Comment on the regime of parameters:	4
B. Velocity variance	5
Velocity variance in Schwinger Keldysh formalism	5
Numerical test	6
IV. Microscopic time reversality of bath and non-linear FDR	6
Velocity four point function in SK formalism	7
A numerical study of non-linear FDR	7
V. Conclusion	8
Acknowledgments	8
A. Noise correlation functions in corrections of parameters	8
Correction to q_a^2 vertex:	8
Correction to $q_a \dot{q}$ vertex:	8
Correction to q_a^4 vertex:	9
Correction to $q_a^3 \dot{q}$ vertex:	9
B. Functional derivation of Schwinger-Keldysh propagators	9

Sub-leading correction to f^r, ζ_η^r due to $\bar{c}c$ loop:

12

References

12

I. INTRODUCTION

A Brownian particle interacting with its thermal bath is successfully described by linear Langevin equation. The particle satisfies (linear) fluctuation-dissipation relation (FDR) which states that the variance of bath fluctuation is directly proportional to linear drag of the bath.

The linear model can be thought of as the leading approximation to a full non-linear Langevin dynamics obtained by adding non-linear correction to the linear one. The non-linear correction can be of various types - it can either be a function of system variables ($F_1(q, \dot{q})$) or a function of the noise ($F_2(\eta)$) or both ($F_3(q, \dot{q}, \eta)$). In this work we focus on the third type, i.e., non-linearity as a function of both noise and system variable. The simplest such second order non-linear Langevin equation [1–4] is given by

$$\mathcal{E}(t) = \ddot{q} + (\gamma + \zeta_\gamma \eta^2) \dot{q} - f \eta = 0. \quad (1)$$

Here q is the particle's position and ' \cdot ' is defined as the time derivative. We have assumed a spatial translational symmetry for simplicity so that we do not have any term involving the position. Here, γ and f are damping coefficient and strength of the thermal noise respectively. The damping coefficient γ is corrected by $\zeta_\gamma \eta^2$ which can be thought of as a thermal jitter in γ with strength ζ_γ . The noise η can no longer be a Gaussian distribution in such a non-linear condition. It has to be drawn from a non-Gaussian distribution [1, 3, 4] as the following.

$$P(\eta) \sim e^{-\delta t \left\{ \frac{f}{2} \eta^2 + \frac{\zeta_\gamma}{4!} \eta^4 \right\}}, \quad (2)$$

* channdann.jana@gmail.com

ζ_η being the strength of quartic noise. To summarise the number of parameters, we have two linear (f, γ) and two non-linear parameters (ζ_η, ζ_γ) present in the theory.

A natural question one might ask, what happens to the FDR provided the noise is non-Gaussian. Another question could be if there exists an FDR-like relation between ζ_η and ζ_γ . The authors of [1, 3, 4] use a Schwinger-Keldysh (SK)[5, 6]¹ path integral description [9–11] of (1) and show that the FDR (linear) is untouched. They find another FDR (non-linear) at the level of non-linear parameters in the weak system-bath coupling regime. However, these relations hold for path integral parameters which are not same as non-linear Langevin parameters. We show in §II that parameters in Langevin and path integral descriptions are related by a renormalisation flow where path-integral parameters are the renormalised/physical ones. The linear and non-linear FDR are given by

$$\gamma^r = \frac{\beta}{2} f^r \quad \text{and} \quad \zeta_\gamma^r = -\frac{\beta}{12} \zeta_\eta^r \quad (3)$$

respectively, where β is the inverse temperature. The r labels correspond to the renormalised parameters. Whereas the linear FDR is guaranteed to exist if the bath is thermal, the non-linear one requires time-reversal invariance of bath along with thermality [1, 2].

The above relations are first motivated in [2], derived in [1] from a microscopic theory and later verified using holography in [3, 4]. In all these cases, the system interacts weakly with its bath such that the bath is in thermal equilibrium and has a time reversal invariance. It does not depend on specific details of the bath, e.g., whether we consider a harmonic bath [1, 2] or strongly interacting [3, 4]. It is also shown that the specific non-linearity considered in (1) can only come from non-linearity from the bath.

We perform a numerical check of the FDRs in this work. It is widely believed from our daily experience that non-linearity should not affect the linear FDR. This means, the velocity variance of a non-linear Brownian particle should saturate to its bath temperature. This turns out to be true in our numerical analysis at least for weak system-bath interaction. Then we study the velocity four point function (equal time) and find that it saturates after some characteristic time. Corresponding to it, we define a quartic deviation of velocity analogous to standard deviation. We show that the quartic deviation thermalises in numerical simulation (by checking against analytical result), only if the non-linear FDR is valid and hence the bath is time reversal invariant [12]. Otherwise, the quartic deviation reaches a steady state [13–17] (and references therein).

There are two steps to arrive at the above results. First one is, we find a renormalisation procedure relating the Langevin parameters to the renormalised parameters appearing in (3), which is essential to establish the linear FDR. This renormalisation procedure seems to have a broader theoretical perspective. It is clear from our analysis that renormalisation should exist in all stochastic processes with higher noise cumulants. The another step is the preparation of non-Gaussian noise with quartic cumulant. We prepare it using a numeric tool called the *rejection sampling*[18]. According to this tool, we can prepare an arbitrary noise distribution from a known distribution.

II. RENORMALISATION OF PARAMETERS IN THE DISCRETISED PROBLEM

The MSR trick establishes an equivalence between SK path integral and stochastic description of a system. This means, each Langevin equation has a SK path integral interpretation - wherein a new fluctuation variable (q_d) plays the role of the noise. The parameters appearing in the SK description are physical, thus we call those as **renormalised** parameters. The parameters appearing in the Langevin equation are related to renormalised ones by renormalisation flow equations. We call those as the **bare** parameters. In this section, we find relations among bare and renormalised parameters.

Following MSR trick [9–11] we find a path integral corresponding to a Langevin equation. The path integral of a particle obeying (1) with noise distribution (2) is given by

$$\begin{aligned} \mathcal{Z} &= \int \mathcal{D}q \mathcal{D}\eta \det \left[\frac{\delta \mathcal{E}}{\delta q} \right] P[\eta] \delta(\mathcal{E}(t)) \\ &= \int \mathcal{D}q \mathcal{D}\eta \mathcal{D}q_d \det \left[\frac{\delta \mathcal{E}}{\delta q} \right] e^{-\int dt \left\{ \left[\frac{f}{2} \eta^2 + \frac{\zeta_\gamma}{4} \eta^4 \right] + i q_d \mathcal{E}(t) \right\}}. \end{aligned} \quad (4)$$

Here q_d is the difference/fluctuation d.o.f. in SK prescription. We follow the Stratonovich convention[19, 20] and write the determinant in (4) as a path integral over two Grassmannian variables (\bar{c}, c) as the following.²

$$\det \left[\frac{\delta \mathcal{E}}{\delta q} \right] = \int \mathcal{D}\bar{c} \mathcal{D}c e^{-i \int dt \bar{c} \left[\frac{d}{dt} + \gamma + \zeta_\gamma \eta^2 \right] c}. \quad (5)$$

According to MSR trick we give a shift to the noise by $\eta \rightarrow \eta + i q_d$. The shifting does not essentially change the path integral:

¹ A textbook treatment of SK formalism and its application to non-equilibrium systems can be found in [7, 8].

² One could have also used the Ito convention [8, 19] and set the

determinant to unity. In doing so we will end up making the ζ_γ term non-local [21] by one time step δt . Correspondingly, the path integral description becomes non-local which is cumbersome to handle.

$$\mathcal{Z} = \int \mathcal{D}q \mathcal{D}\eta \mathcal{D}q_d \mathcal{D}\bar{c} \mathcal{D}c e^{-\int dt \left\{ \left[\frac{f}{2}(\eta+iq_d)^2 + \frac{\zeta_\eta}{4!}(\eta+iq_d)^4 \right] + iq_d \mathcal{E}(t) + i\bar{c} \left[\frac{d}{dt} + \gamma + \zeta_\gamma(\eta+iq_d)^2 \right] c \right\}}. \quad (6)$$

Then we integrate out the noise by computing noise-noise correlation functions. Since there is non-Gaussianity in the noise distribution, we can only inte-

grate out the noise perturbatively. The path integral in terms of noise correlation functions takes the following form in perturbation theory.

$$\begin{aligned} \mathcal{Z} = & \int \mathcal{D}q \mathcal{D}q_d \mathcal{D}\bar{c} \mathcal{D}c e^{-\int dt \left[\frac{f}{2}q_d^2 + \frac{\zeta_\eta}{4!}q_d^4 + iq_d(\ddot{q} + (\gamma - \zeta_\gamma q_d^2)\dot{q}) + i\bar{c} \left(\frac{d}{dt} + \gamma - \zeta_\gamma q_d^2 \right) c \right]} \\ & \left\{ 1 + \int dt \left[\frac{\zeta_\eta}{2!2!} \langle \eta^2 \rangle q_d^2 - i\zeta_\gamma \langle \eta^2 \rangle q_d \dot{q} - i\zeta_\gamma \langle \eta^2 \rangle \bar{c} c \right] + \frac{i\zeta_\gamma \zeta_\eta}{4!} \int dt dt' \langle \eta^4(t') \eta^2(t) \rangle q_d(t) \dot{q}(t) \right. \\ & - \frac{\zeta_\eta^2}{4!} \int dt dt' \left[\frac{1}{2^2} \langle \eta^2(t) \eta^4(t') \rangle q_d^2(t) + \frac{1}{3} \langle \eta^3(t) \eta^3(t') \rangle q_d(t) q_d(t') \right] \\ & + \frac{\zeta_\eta^2}{4!} \int dt dt' \left[\frac{2}{3} \langle \eta(t) \eta^3(t') \rangle q_d^3(t) q_d(t') + \frac{3}{4} \langle \eta^2(t) \eta^2(t') \rangle q_d^2(t) q_d^2(t') \right] \\ & - i\zeta_\gamma \zeta_\eta \int dt dt' \left[\frac{1}{3} \langle \eta(t) \eta^3(t') \rangle q_d^2(t) \dot{q}(t) q_d(t') + \frac{1}{4} \langle \eta^2(t) \eta^2(t') \rangle q_d^2(t) q_d(t') \dot{q}(t') \right] \\ & \left. - i\zeta_\gamma \zeta_\eta \int dt dt' \left[\frac{1}{4} \langle \eta^2(t) \eta^2(t') \rangle \bar{c}(t) c(t) q_d^2(t') + \frac{1}{3} \langle \eta(t) \eta^3(t') \rangle \bar{c}(t) c(t) q_d(t) q_d(t') \right] + \dots \right\}. \quad (7) \end{aligned}$$

Note that, in the Taylor expanded form, we have kept terms till quartic order(in q, q_d, \bar{c}, c). The higher order terms are suppressed due to small non-linear couplings. The noise correlation functions are UV divergent; thus we put a UV cut-off δt in time which also acts as the

smallest time step in the discretised problem discussed through out this paper.

We evaluate various noise correlation functions of (7) in appendix A. With the noise correlation function, we exponentiate the RHS of (7) back and find the following effective path integral.

$$\mathcal{Z} = \int \mathcal{D}q \mathcal{D}q_d \mathcal{D}\bar{c} \mathcal{D}c \times \exp \left[- \int dt \left\{ iq_d \ddot{q} + i\gamma^r q_d \dot{q} + \frac{f^r}{2} q_d^2 + i\bar{c} \left(\frac{d}{dt} + \gamma - \zeta_\gamma q_d^2 \right) c + \zeta_\eta^r \frac{q_d^4}{4!} - i\zeta_\gamma^r q_d^3 \dot{q} + \dots \right\} \right]. \quad (8)$$

The r labelled parameters are renormalised parameters (evaluated in appendix A) and are given by

$$f^r = f - \frac{\zeta_\eta}{2f\delta t} + \frac{2\zeta_\eta^2}{3f^3(\delta t)^2} + \dots, \quad (9a)$$

$$\gamma^r = \gamma + \frac{\zeta_\gamma}{f\delta t} - \frac{\zeta_\gamma \zeta_\eta}{2f^3(\delta t)^2} + \dots, \quad (9b)$$

$$\zeta_\eta^r = \zeta_\eta - \frac{7}{2} \frac{\zeta_\eta^2}{f^2\delta t} + \frac{149}{12} \frac{\zeta_\eta^3}{f^4(\delta t)^2} + \dots, \quad (9c)$$

$$\zeta_\gamma^r = \zeta_\gamma - \frac{3\zeta_\eta \zeta_\gamma}{2f^2\delta t} + \frac{10}{3} \frac{\zeta_\eta^2 \zeta_\gamma}{f^4(\delta t)^2} + \dots. \quad (9d)$$

Here δt is the UV cut-off and the smallest time step and the perturbation parameter is $\sim \frac{\zeta_\eta}{f^2\delta t}$. Note that the front factors, in RHS of the above relations, are larger

down the series. So, we choose the bare parameters such that perturbation theory is valid. The parameters corresponding to the Grassmann variables \bar{c}, c also obtain correction from noise correlation function, but those can be neglected due to the following reason. Since, \bar{c} and c do not constitute any physical observable due to their Grassmannian nature, they do not have any direct contribution in any correlation function; they only have sub-leading loop contribution. So, the leading parameters corresponding to Grassmann vertices in (8) make sub-leading contribution to correlation function. Hence noise loop correction to those parameters will be sub-sub-leading and thus are ignored (see appendix B).

One might be concerned about LHS of (9) being called as renormalised parameters, since they may receive correction due to quartic terms in (8) and be further renor-

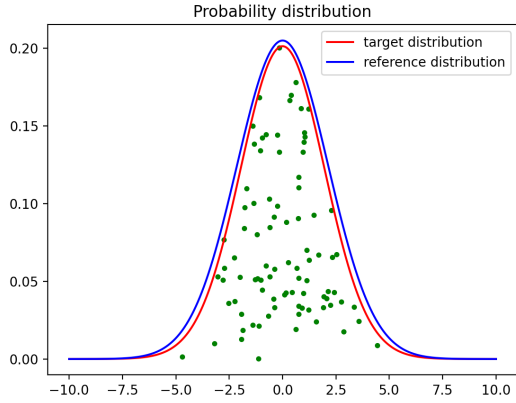


FIG. 1: The target distribution P is found from the known reference distribution P_g . P_g is chosen to be a scaled Gaussian distribution whose exact form is not relevant; it only has to contain the full target distribution. The target distribution $P(\eta) \sim e^{-\delta t \left(\frac{f}{2} \eta^2 + \frac{\zeta_\eta}{4!} \eta^4 \right)}$. The green dots generated from the rejection sampling, plot $u \times P_g$. Note that these dots do not go out of the red curve.

malised. We will argue in §III B that the renormalised parameters are not further corrected by ζ_γ^r or ζ_η^r interactions. Although we get \bar{c} -loop corrections but those are sub-leading as discussed above. Therefore we can safely call LHS of (9) as the renormalised parameters.

The bare parameters in (9), according to the notion of renormalisation, should flow with δt whereas the renormalised parameters are fixed by the system itself. This means that the bare parameters can take different values along the flow depending on δt . One can find the flow equations by writing the bare parameters in terms of the renormalised ones, which can be found easily by making suitable approximation.

III. PREPARATION OF NOISE AND PARTICLE CORRELATION FUNCTIONS

In this section, we describe the preparation of non-Gaussian noise. Then we solve the non-linear Langevin equation numerically and compute relevant correlators. Although we do not have a complete analytic handle on

the non-linear dynamics, we can still compute the saturation value of correlation functions and match with numerical data.

A. Preparation of noise

We prepare the non-Gaussian noise distribution $P(\eta)$ in (2) from a reference Gaussian distribution by a method called **rejection sampling**³[18] originally proposed by von Neumann. (One could use different numerical methods such as Metropolis Hastings [22]). According to rejection sampling, we choose a reference noise distribution (Gaussian) function $P_g(\eta)$. The reference distribution $P_g(\eta)$ need not be normalised and should be such that it contains the full target distribution $P(\eta)$ within, as shown in figure 1. Then we choose a random number u between $[0, 1]$. If $u < \frac{P(\eta)}{P_g(\eta)}$ for a generated η from P_g , we keep that η for P ; else we discard. By repeating this process many times we can generate P . Out of 100 iteration figure 1 plots those data which follow the above inequality. An infinite number of iteration should populate the entire target distribution.

It is worthwhile to point out a subtlety in the target noise distribution $P(\eta)$. A holographic derivation [3, 4] of the non-linear Langevin equation finds that the actual numerical value of ζ_η is negative which makes $P(\eta)$ ill defined since it diverges as $\eta \rightarrow \infty$. To stabilise it, we add a small regulator such that the regulated distribution is given by

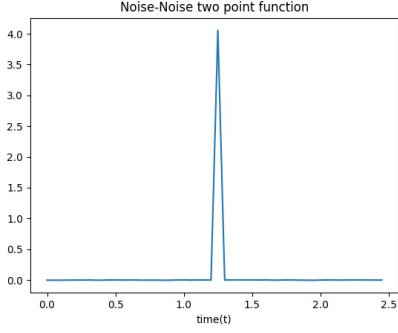
$$P_{\text{regulated}}(\eta) \sim e^{-\delta t \left(\frac{f}{2} \eta^2 + \frac{\zeta_\eta}{4!} \eta^4 + \epsilon \eta^6 \right)}, \quad 1 \gg \epsilon > 0. \quad (10)$$

The justification of the above regulator could be the following. All derivations of the Langevin equation consider only the leading order influence phase [23] from the bath. The sub-leading correction should stabilise the distribution to make it a sensible theory. We choose ϵ such that it nullifies any sixth cumulant generated during the noise preparation. We generate sufficient number (10^8) of η using rejection sampling and plot the noise correlation functions in figure 2 which shows a sharp peak for the quadratic and quartic cumulants but only fluctuations for the sixth cumulant. Since we have successfully prepared the noise, we are ready to study the particle's dynamics.

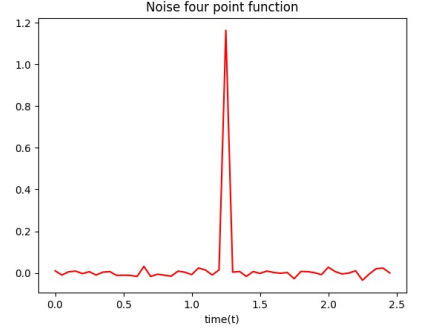
Comment on the regime of parameters:

The bare parameters given in (1) are used in the numerical computation whereas the renormalised ones are used in the analytics. The renormalised parameters are related to the bare parameters by an infinite series as written in (9). We evaluate till second order noise loop corrections in this series. This means our choice of bare parameters should be such that the convergence is fast enough to ensure matching of numeric and analytic data.

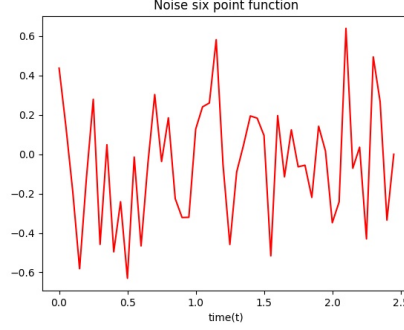
³ I thank Anugu Sumith Reddy for bringing the rejection sampling method to my notice.



(a) Noise two point function



(b) Noise four point function



(c) Noise six point function

FIG. 2: We compute $\langle \eta(t)\eta(1.25) \rangle$, $\langle \eta(t)\eta(1.25)^3 \rangle$ and $\langle \eta(t)\eta(1.25)^5 \rangle$ in figure 2a, 2b and 2c respectively. Since the noise does not have any dynamics, we get a peak (non-zero correlation) only when time of all noise variable are equal. The parameters for non-Gaussian noise distribution are chosen as $f = 5.11$ and $\zeta_\eta = -0.086$ which are also the bare parameters discussed in §II. The six point function in 2c is essentially indistinguishable from the fluctuation. The number of iteration for each graph is 10^7 .

We choose the bare parameters and the time step as

$$f = 5.11, \quad \zeta_\eta = -0.086 \quad \text{and} \quad \delta t = 0.05 \quad (11)$$

respectively so that the perturbation parameter $\frac{\zeta_\eta}{f^2 \delta t} (= 0.066)$ in (9) makes the second order term small (compared to the fast order term).

Let us now ask the following question. How much can we deviate from (11) - the values of individual bare parameters, keeping the perturbation parameter at same order? If we make each parameter larger then the Euler-Maruyama error grows due to large values of f and δt . Thus we will find deviation from analytic results. On the other hand, if we make each parameter smaller than in (11), we observe the following. We may get rid of the Euler-Maruyama error, but small f and δt bring large fluctuation in higher cumulants. For example, for $f = 1$, $\zeta_\eta = -0.001$ and $\delta t = 0.5$, 5×10^8 number of ensemble is insufficient to tame the fluctuation and get a definitive plot for connected velocity four point function defined in (23). Thus we conclude that we should not make the parameters too large or too small. However, if one gets improvements on either side by better numerical methods, then the domain of validity of parameters can be made bigger.

B. Velocity variance

The velocity variance of a Brownian particle in a thermal bath saturates after some time evolution and according to linear FDR, the saturation value is equal to the temperature of the bath. In this section, we numerically compute the velocity variance for non-linear Langevin equation and show that its velocity variance exactly matches with the linear one at same temperature. We also perform an analytic check on the saturation value using SK formalism.

Velocity variance in Schwinger Keldysh formalism

Velocity two point correlations for a generic initial condition are hard to compute. But, the corresponding thermal correlations can be found in SK formalism, which can be used to verify the numerical data. Thus, we compute the thermal SK propagators (appendix B) and thereafter relevant correlation functions with the help of propagators and vertex factors. The SK propagators are given

by

$$G^K(t_1, t_2) \equiv \langle \dot{q}(t_2) \dot{q}(t_1) \rangle = \frac{f^r}{2\gamma^r} e^{-\gamma^r |t_2 - t_1|}, \quad (12)$$

$$G^A(t_1, t_2) \equiv \langle q_d(t_2) \dot{q}(t_1) \rangle = -i \Theta(t_1 - t_2) e^{-\gamma^r (t_1 - t_2)} \quad (13)$$

$$G^R(t_1, t_2) \equiv \langle \dot{q}(t_2) q_d(t_1) \rangle = -i \Theta(t_2 - t_1) e^{-\gamma^r (t_2 - t_1)} \quad (14)$$

$$\langle q_d(t_2) q_d(t_1) \rangle = 0. \quad (15)$$

Here, \dot{q} is the particle's velocity and q_d , as discussed in §II, can be thought of as a dual variable corresponding to noise η . The above non-zero propagators are the Keldysh, advanced and the retarded propagators respectively. The absence of the fourth propagator restricts us to construct any loop consisting of q_d, \dot{q} with the available interaction terms in (8). However there will be Grassmanian loop corrections. These corrections are negligibly small, thus can be neglected (see appendix B). So, in absence of non-linear correction, the above thermal propagators in (12) are nothing but correlation functions. In particular the Keldysh propagator is the velocity two point function and at equal time is the velocity variance given by $\frac{f^r}{2\gamma^r}$.

Numerical test

In order to study the dynamics of (1), we discretise it as the following.

$$q(t + \delta t) = q(t) + \delta t \dot{q},$$

$$\dot{q}(t + \delta t) = \dot{q}(t) + \delta t (\gamma + \zeta_\gamma (\eta(t))^2) \dot{q}(t) = f \delta t \eta(t). \quad (16)$$

The key point is that the parameters in the above equation are bare parameters. With these parameters we plot variance of velocity of the particle in figure 3. In this figure, we also simulate the linear Langevin equation with renormalised linear couplings (f^r, γ^r) and find that the velocity variances in both cases match. One might argue, discrepancy between them in figure 3 are not observed due to weak system-bath coupling and thus there is no significant distinction between bare and renormalised parameters. This is not correct. Had we used bare linear parameters (f, γ) and made $\zeta_\eta, \zeta_\gamma = 0$ in (1), we would have got the dashed curve. So, the non-linear couplings do make a significant contribution.

IV. MICROSCOPIC TIME REVERSALITY OF BATH AND NON-LINEAR FDR

The non-linear FDR, as discussed in the introduction, seems to be generic from the discussions of [1, 2] and [3]. In [1, 2], non-linear FDR was derived assuming weak non-linear system-bath interaction. On the other hand, [3] found an identical FDR with linear system-bath interaction where the bath being non-linear and strongly coupled. Thus non-linear FDR does not seem to depend

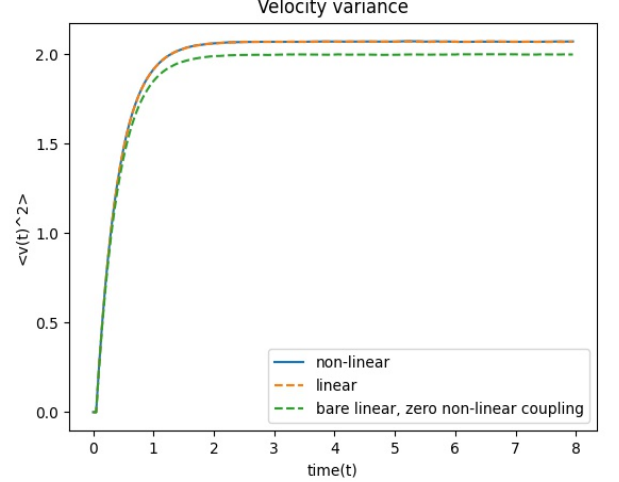


FIG. 3: The bare parameters are given by $f = 5.11$, $\gamma = 1.31$, $\zeta_\eta = -0.086$, $\zeta_\gamma = 0.0042$. The corresponding renormalised parameters are evaluated from (9) as $f^r = 5.29$, $\gamma^r = 1.32$, $\zeta_\eta^r = -0.112$ and $\zeta_\gamma^r = 0.0046$ for $\delta t = 0.05$. We assume both initial position and momentum as zero and find that velocity variance exactly matches in both linear and non-linear cases. Notice that saturation value does not occur exactly at $T = \frac{f^r}{2\gamma^r} = 2$ due to the Euler-Maruyama error. We have chosen $f, \delta t$ large enough that the error is noticeable. However, since we are matching with linear Langevin result which also have identical error, the apparent deviation is irrelevant. The dashed line plots velocity variance with bare linear parameters but zero non-linear parameters. The number of iteration for each curve is 10^7 .

on the details of bath, rather it depends on a generic principle: microscopic time reversal invariance of the bath.

Microscopic time reversality of bath, in general, imposes certain constraints on the system's effective theory. These relations were first discovered by Onsager [24, 25] and extended by Casimir [26] in the context of a system with multiple degrees of freedom. According to this observation, if a) the bath Hamiltonian H_B commutes with the time reversal operator \mathbf{T} and b) the bath operator \mathcal{O} , through which the bath interacts with the system, is even under time reversal:

$$[\mathbf{T}, H_B] = 0, \quad \mathbf{T}^{-1} \mathcal{O}(t) \mathbf{T} = \mathcal{O}(-t), \quad (17)$$

then certain parameters in the system's effective theory are related.

Following [1, 2], we motivate the above assertion in the context of non-linear FDR by considering the following bath four point function:

$$\langle \mathcal{O}(t_1) \mathcal{O}(t_2) \mathcal{O}(t_3) \mathcal{O}(t_4) \rangle. \quad (18)$$

This kind of four point functions would appear in the influence phase of the effective theory when we integrate

out the bath perturbatively. Due to time reversal invari-

ance we have

$$\langle \mathcal{O}(t_1)\mathcal{O}(t_2)\mathcal{O}(t_3)\mathcal{O}(t_4) \rangle = \langle \mathbf{T}^\dagger \mathcal{O}(t_1)\mathcal{O}(t_2)\mathcal{O}(t_3)\mathcal{O}(t_4)\mathbf{T} \rangle^* \quad (19)$$

Using time reversal (17) and hermiticity of \mathcal{O} , we get

$$\langle \mathcal{O}(t_1)\mathcal{O}(t_2)\mathcal{O}(t_3)\mathcal{O}(t_4) \rangle = \langle \mathcal{O}(-t_1)\mathcal{O}(-t_2)\mathcal{O}(-t_3)\mathcal{O}(-t_4) \rangle^* = \langle \mathcal{O}(-t_4)\mathcal{O}(-t_3)\mathcal{O}(-t_2)\mathcal{O}(-t_1) \rangle \quad (20)$$

Let us choose $t_1 = t_4 = 0$ and $t_2 = t_3 = t$. Then we get

$$\langle \mathcal{O}(0)\mathcal{O}(t)\mathcal{O}(t)\mathcal{O}(0) \rangle = \langle \mathcal{O}(0)\mathcal{O}(-t)\mathcal{O}(-t)\mathcal{O}(0) \rangle. \quad (21)$$

Note that the LHS is a SK correlation function for $t > 0$ since it can be captured in SK contour [8, 27]. But the RHS does not belong to SK correlation - it is rather an out-of-time-ordered (OTO) correlation function. (A review on generalised OTO correlation can be found in [28–30].) Now, we impose thermality on the RHS via the KMS relation and find

$$\langle \mathcal{O}(0)\mathcal{O}(t)\mathcal{O}(t)\mathcal{O}(0) \rangle = \langle \mathcal{O}(-i\beta)\mathcal{O}(0)\mathcal{O}(-t)\mathcal{O}(-t) \rangle. \quad (22)$$

Thus we find that two different SK correlation functions are related by both time-reversal invariance and thermal-ity. When we integrate out the bath then bath correlations at the system time scale appears as parameters in the effective theory. Thus from (22), we expect to get certain relation between corresponding parameters. This motivates the idea of why should there be a non-linear FDR under time reversal invariance and thermal nature of the bath.

Velocity four point function in SK formalism

With the above motivation in the starting of this section, it is worthwhile to study the non-linear FDR which relates two quartic terms in the effective path-integral (8). In this section, we compute connected part of the velocity four point function defined as

$$\langle \dot{q}^4(t) \rangle_c = \langle \dot{q}(t)^4 \rangle - 3\langle \dot{q}^2(t) \rangle^2. \quad (23)$$

The SK effective action defined as the argument of exponential in (8), is simple enough to have only Grassmannian loop correction to all coupling constants. One can perform an explicit check that only Grassmannian loop can be formed provided $\langle q_d(t_1)q_d(t_2) \rangle = 0$. The Grassmannian loops are sub-leading as pointed out in §B. Therefore we consider only tree level contribution evaluated below.

The tree level correlator for (23) gets contribution from

both ζ_η^r and ζ_γ^r terms, given by

$$\begin{aligned} \langle \dot{q}^4(t) \rangle_c &= -\zeta_\eta^r \int dt' \langle \dot{q}(t)q_d(t') \rangle^4 \\ &\quad + (4!i\zeta_\gamma^r) \int dt' \langle \dot{q}(t)q_d(t') \rangle^3 \langle \dot{q}(t')\dot{q}(t) \rangle \quad (24) \\ &= -\frac{\zeta_\eta^r}{4\gamma^r} - 4! \frac{\zeta_\gamma^r}{4\gamma^r} = \frac{\zeta_\eta^r}{4\gamma^r}, \end{aligned}$$

where in the last expression we have used the non-linear FDR from (3). Note that the velocity four point function is a negative quantity. Thus we define a quartic deviation (analogous to standard deviation) of velocity as the following:

$$v_{QD} \equiv -|\langle \dot{q}^4(t) \rangle_c|^{1/4}. \quad (25)$$

We check the above expression numerically in the following.

A numerical study of non-linear FDR

We find numerically the connected velocity four point function defined in (23) for 4×10^7 iterations. However, due to our choice of parameters, velocity four point function is comparable to typical fluctuation for the above number of iteration. We can reduce the fluctuation substantially by taking a fourth root of the velocity four point function as the following.

$$v_{QD}(t)|_{\text{numeric}} \equiv \begin{cases} (\langle \dot{q}^4(t) \rangle_c)^{1/4}, & \text{if } \langle \dot{q}^4(t) \rangle_c > 0 \\ -|\langle \dot{q}^4(t) \rangle_c|^{1/4}, & \text{if } \langle \dot{q}^4(t) \rangle_c < 0 \end{cases} \quad (26)$$

The above definition for numerical analysis is different from (25) due to our prior ignorance about the sign of $\langle \dot{q}^4(t) \rangle_c$ in numerical analysis. We plot the above quantity in figure 4 and find that the saturation value of the numerical data matches quite well with the analytic result. Thus we conclude that the quartic deviation is given

$$\text{by } v_{QD} = -\left| \frac{\zeta_\eta^r}{4\gamma^r} \right|^{1/4}.$$

In figure 4, there is a bump during the initial time evolution. To understand this feature, let us consider the discretised non-linear Langevin equation (16) at $t = 0$. Since the initial velocity is zero, there is no ζ_γ contribution at $t = 0$. But we still have a ζ_η contribution from

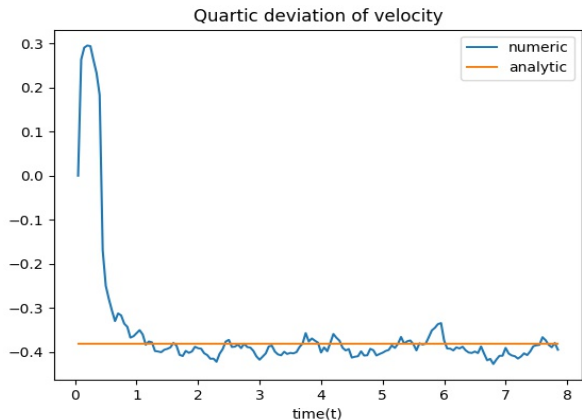


FIG. 4: We plot the quartic deviation $v_{QD}(t)$ defined in (26) for 4×10^7 number of iterations. The analytic result is only the thermalised value. We have chosen the initial velocity as zero.

the noise which has a positive cumulant. Thus we get a positive bump at $t = \delta t$. After a few more time-steps ζ_γ term takes over since it has a larger negative contribution as pointed out in (24).

Let us now break the time reversal invariance artificially by introducing a deviation parameter α defined as

$$\zeta_{\gamma \text{ dev}}^r \equiv \alpha \frac{-\zeta_\eta^r}{12}. \quad (27)$$

We plot (26) in figure 5 for different values of α and find that the numeric and analytic data do not agree for $\alpha \neq 1$. The interpretation of this disagreement is the following. If the time reversal invariance of bath is broken ($\alpha \neq 1$), then we do not expect the particle to thermalise [12–17]. Rather, in our case, it reaches a steady state. The numerical data in figure 5 thus produce the steady state values at late time. On the other hand, the analytic results are derived assuming thermal SK propagators of the particle, even though we use (27) in analytic evaluation of quartic deviation. As a result, the numeric and analytic results does not match - they agree only when the correct non-linear FDR is used. Thus we conclude that the non-linear FDR is a valid relation for thermal equilibration.

V. CONCLUSION

This work deals with systematic analysis of non-linear Langevin equation in presence of non-Gaussian noise. We show how the non-Gaussianity introduces the notion of renormalisation such that the bare/unphysical parameters are the parameters appearing in Langevin equation. On the other hand the renormalised/physical parameters appear in the Schwinger-Keldysh effective action. We show, the bare and renormalised parameters are related by noise loop correction.

In the second half of this work, we do a numerical analysis to find the velocity variance and velocity four point function. With the help of two point correlations, we show that the linear FDR is valid for non-linear Langevin dynamics in presence of weak system-bath interaction. We find excellent agreement of velocity variance between linear and non-linear Langevin dynamics. We compute velocity four point function numerically and show that it agrees with thermal velocity four point function (calculated analytically) when non-linear FDR is satisfied. This is a signature of thermalisation. When we deviate from the non-linear FDR, then the system does not thermalise but settles to a steady state.

ACKNOWLEDGMENTS

I would like to thank Soumyadeep Chaudhuri for initial collaboration and guidance. I thank Arghya Das, Anupam Kundu, R. Loganayagam, Ajit Mehta, Avaya Pal, Archak Purkayastha, Anugu Sumith Reddy, Arnab Rudra, Prashant Singh, Rahul Singh and Akhil Sivakumar for useful suggestions.

Appendix A: Noise correlation functions in corrections of parameters

We consider the path integral in (7) which evaluates correction to all parameters. To evaluate the loop diagrams we need the noise propagator as a Feynman rule. Since the noise does not have any dynamics, the propagator can only be Dirac-Delta function of time. But, in our numerical analysis, since the smallest available time scale is the time step δt , we write the following expression for noise propagator.

$$\langle \eta(t_1) \eta(t_2) \rangle = \begin{cases} \frac{1}{f \delta t} & \text{if } t_1 = t_2 \\ 0 & \text{else.} \end{cases} \quad (A1)$$

The corresponding diagrammatic representation is given in figure 6.

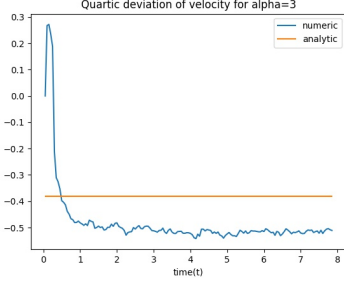
Correction to q_d^2 vertex:

The correction to f are obtained from the noise two loop diagrams drawn in figure 7. The correction to f is also pointed out below each diagram. Adding all the contributions we get

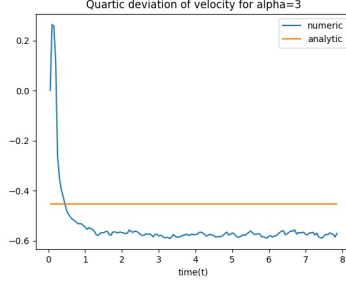
$$f^r = f - \frac{\zeta_\eta}{2f \delta t} + \frac{2\zeta_\eta^2}{3f^3(\delta t)^2} \quad (A2)$$

Correction to $q_d \dot{q}$ vertex:

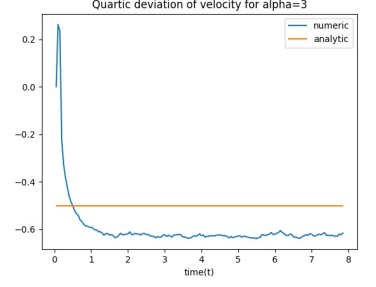
The diagrams which contribute to $q_d \dot{q}$ vertex are drawn in figure 8.



(a) Quartic deviation of velocity for $\alpha = 2$.



(b) Quartic deviation of velocity for $\alpha = 3$.



(c) Quartic deviation of velocity for $\alpha = 4$.

FIG. 5: We compute v_{QD} for deviated FDR defined in (27). Note that the analytic results differ from the numerical data.

$$\overline{t} \quad t : \quad \langle \eta(t) \eta(t) \rangle = \frac{1}{f \delta t}$$

FIG. 6: Diagrammatic representation of noise propagator

Adding all contribution we get the following expression for γ^r .

$$\gamma^r = \gamma + \frac{\zeta_\gamma}{f \delta t} - \frac{\zeta_\gamma \zeta_\eta}{2 f^3 (\delta t)^2}. \quad (\text{A3})$$

Correction to q_d^4 vertex:

The correction to q_d^4 vertex gets contribution from the diagrams shown in figure 9. Combining all of these correction we get the renormalised ζ_η^r as

$$\zeta_\eta^r = \zeta_\eta - \frac{7}{2} \frac{\zeta_\eta^2}{f^2 \delta t} + \frac{149}{12} \frac{\zeta_\eta^3}{f^4 (\delta t)^2}. \quad (\text{A4})$$

Correction to $q_d^3 \dot{q}$ vertex:

The correction to $q_d^3 \dot{q}$ vertex gets contribution from the diagrams shown in figure 10. Combining all of these correction we get the renormalised ζ_γ^r as

$$\zeta_\gamma^r = \zeta_\gamma - \frac{3 \zeta_\eta \zeta_\gamma}{2 f^2 \delta t} + \frac{10}{3} \frac{\zeta_\eta^2 \zeta_\gamma}{f^4 (\delta t)^2}. \quad (\text{A5})$$

Appendix B: Functional derivation of Schwinger-Keldysh propagators

The propagators are obtained by considering the quadratic part of path-integral (8). Then we introduce sources corresponding to all variables. The propagators for a generic initial condition is hard to compute. However, we can compute the thermal propagators. We shift the variables and finally take functional derivative of the path integral w.r.t. the sources and obtain the thermal propagators. The quadratic path integral with the sources is given by

$$\begin{aligned} Z_0[J_{\dot{q}}, J_d, J_c, J_{\bar{c}}] &= \int \mathcal{D}\dot{q} \mathcal{D}q_d \mathcal{D}\bar{c} \mathcal{D}c \exp \left[- \int dt \{ J_{\dot{q}} \dot{q}_d + J_d \dot{q} + J_c c + \bar{c} J_{\bar{c}} \} \right] \\ &\times \exp \left[- \int dt \left\{ i q_d \ddot{q} + i \gamma^r q_d \dot{q} + \frac{f^r}{2} q_d^2 + i \bar{c} \left(\frac{d}{dt} + \gamma \right) c \right\} \right]. \end{aligned} \quad (\text{B1})$$

Here $J_{\dot{q}}$, J_d , J_c and $J_{\bar{c}}$ are sources of q_d , \dot{q} , c and \bar{c} respectively. It may seem that q_d and \dot{q} sources are flipped.

But, it is a convention followed in SK literature. The path integral in Fourier space

$$\begin{aligned} Z_0 &= \int \mathcal{D}\dot{q} \mathcal{D}q_d \mathcal{D}\bar{c} \mathcal{D}c \times \exp \left[- \int \frac{d\omega}{2\pi} \left\{ \tilde{J}_{\dot{q}}(-\omega) \tilde{q}_d(\omega) + \tilde{J}_d(-\omega) \tilde{q}(\omega) + \tilde{J}_c(-\omega) \tilde{c}(\omega) + \tilde{\bar{c}}(-\omega) \tilde{J}_{\bar{c}}(\omega) \right\} \right] \\ &\times \exp \left[- \int \frac{d\omega}{2\pi} \left\{ \tilde{q}_d(-\omega) (\omega + i \gamma^r) \tilde{q} + \frac{f^r}{2} \tilde{q}_d(-\omega) \tilde{q}_d(\omega) + \tilde{\bar{c}}(-\omega) (\omega + i \gamma) \tilde{c}(\omega) \right\} \right]. \end{aligned} \quad (\text{B2})$$

$$\begin{aligned} \text{Diagram 1} &= \text{Diagram 2} + \text{Diagram 3} + \text{Diagram 4} + \text{Diagram 5} + \text{Diagram 6} \\ -\frac{f^r}{2} &= -\frac{f}{2} + \frac{1}{4} \frac{\zeta_\eta}{f\delta t} - \frac{1}{12} \frac{\zeta_\eta^2}{f^3\delta t^2} - \frac{1}{8} \frac{\zeta_\eta^2}{f^3\delta t^2} - \frac{1}{8} \frac{\zeta_\eta^2}{f^3\delta t^2} \end{aligned}$$

FIG. 7: Loop correction to q_d^2 vertex in SK path integral (7). The corrected parameter is the renormalised parameter.

$$\begin{aligned} \text{Diagram 1} &= \text{Diagram 2} + \text{Diagram 3} + \text{Diagram 4} \\ -i\gamma^r &= -i\gamma + \frac{-i\zeta_\gamma}{f\delta t} + \frac{i}{2} \frac{\zeta_\gamma \zeta_\eta}{f^3\delta t^2} \end{aligned}$$

FIG. 8: Loop correction to $q_d \dot{q}$ vertex in SK path integral (7).

We give a shift to the variables as the following such that the variables and their corresponding sources are

decoupled.

$$\tilde{q}'_d(\omega) = \tilde{q}_d(\omega) + \frac{\tilde{J}_d(\omega)}{-\omega + i\gamma^r}, \quad (\text{B3})$$

$$\tilde{q}'(\omega) = \tilde{q}(\omega) - \frac{f^r \tilde{J}_d(\omega)}{(-\omega + i\gamma^r)(\omega + i\gamma^r)} + \frac{\tilde{J}_q(\omega)}{\omega + i\gamma^r}, \quad (\text{B4})$$

$$\tilde{c}'(\omega) = \tilde{c}(\omega) + \frac{\tilde{J}_{\bar{c}}(\omega)}{\omega + i\gamma}, \quad (\text{B5})$$

$$\tilde{c}'(\omega) = \tilde{c}(\omega) + \frac{\tilde{J}_c(\omega)}{-\omega + i\gamma}. \quad (\text{B6})$$

The corresponding path-integral is given by

$$\begin{aligned} \mathcal{Z}_0 &= \int \mathcal{D}\dot{q}' \mathcal{D}q'_d \mathcal{D}\tilde{c}' \mathcal{D}c' \exp \left[\int \frac{d\omega}{2\pi} \left\{ \frac{f^r}{2} \frac{\tilde{J}_d(-\omega) \tilde{J}_d(\omega)}{\omega^2 + (\gamma^r)^2} - \frac{\tilde{J}_q(-\omega) \tilde{J}_d(\omega)}{\omega - i\gamma^r} + \frac{\tilde{J}_c(-\omega) \tilde{J}_{\bar{c}}(\omega)}{\omega + i\gamma} \right\} \right] \\ &\times \exp \left[- \int \frac{d\omega}{2\pi} \left\{ \frac{f^r}{2} \tilde{q}'_d(-\omega) \tilde{q}'_d(\omega) + (\omega + i\gamma^r) \tilde{q}'_d(-\omega) \tilde{q}'(\omega) + (\omega + i\gamma) \tilde{c}'(-\omega) \tilde{c}'(\omega) \right\} \right]. \end{aligned} \quad (\text{B7})$$

The first line in the above expression consists of only sources and the second line does not involve any source.

Thus, integrating out the second line gives a constant which can be absorbed into the definition of \mathcal{Z}_0 . Thus we find

$$\mathcal{Z}_0 = \exp \left[\int \frac{d\omega}{2\pi} \left\{ \frac{f^r}{2} \frac{\tilde{J}_d(-\omega) \tilde{J}_d(\omega)}{\omega^2 + (\gamma^r)^2} - \frac{\tilde{J}_q(-\omega) \tilde{J}_d(\omega)}{\omega - i\gamma^r} + \frac{\tilde{J}_c(-\omega) \tilde{J}_{\bar{c}}(\omega)}{\omega + i\gamma} \right\} \right]. \quad (\text{B8})$$

Fourier transforming back to real time, we get

$$\mathcal{Z}_0 = \exp \left[\int dt_1 dt_2 \int \frac{d\omega}{2\pi} e^{-i\omega(t_2-t_1)} \left\{ \frac{f^r}{2} \frac{J_d(t_2) J_d(t_1)}{\omega^2 + (\gamma^r)^2} - \frac{J_q(t_2) J_d(t_1)}{\omega - i\gamma^r} + \frac{J_c(t_2) J_{\bar{c}}(t_1)}{\omega + i\gamma} \right\} \right] \quad (\text{B9})$$

$$\begin{aligned}
\boxtimes &= \times + \text{[1-loop bubble]} + \text{[1-loop tadpole]} + \text{[2-loop bubble]} + \text{[2-loop tadpole]} \\
-\frac{1}{4!}\zeta_\eta^r &= -\frac{1}{4!}\zeta_\eta + \frac{3}{2 \times 4!} \frac{\zeta_\eta^2}{f^2 \delta t} + \frac{2}{4!} \frac{\zeta_\eta^2}{f^2 \delta t} - \frac{3}{2 \times 4!} \frac{\zeta_\eta^3}{f^4 \delta t^2} - \frac{3}{4 \times 4!} \frac{\zeta_\eta^3}{f^4 \delta t^2} \\
&+ \text{[2-loop bubble]} + \text{[2-loop tadpole]} + \text{[2-loop bubble]} + \text{[2-loop tadpole]} \\
&- \frac{2}{3 \times 4!} \frac{\zeta_\eta^3}{f^4 \delta t^2} - \frac{1}{4!} \frac{\zeta_\eta^3}{f^4 \delta t^2} - \frac{1}{4!} \frac{\zeta_\eta^3}{f^4 \delta t^2} - \frac{3}{4!} \frac{\zeta_\eta^3}{f^4 \delta t^2} \\
&+ \text{[2-loop bubble]} + \text{[2-loop tadpole]} \\
&- \frac{3}{4!} \frac{\zeta_\eta^3}{f^4 \delta t^2} - \frac{3}{2 \times 4!} \frac{\zeta_\eta^3}{f^4 \delta t^2}
\end{aligned}$$

FIG. 9: Loop correction to q_d^4 vertex in SK path integral (7). The sixth 2-loop diagram contains two topologically distinct diagrams which have reflection symmetry.

$$\begin{aligned}
\boxtimes &= \times + \text{[1-loop bubble]} + \text{[1-loop tadpole]} + \text{[2-loop bubble]} + \text{[2-loop tadpole]} \\
i\zeta_\gamma^r &= i\zeta_\gamma - \frac{i}{2} \frac{\zeta_\gamma \zeta_\eta}{f^2 \delta t} - i \frac{\zeta_\gamma \zeta_\eta}{f^2 \delta t} + \frac{i}{2} \frac{\zeta_\eta \zeta_\gamma^2}{f^4 \delta t^2} + \frac{i}{4} \frac{\zeta_\eta \zeta_\gamma^2}{f^4 \delta t^2} \\
&+ \text{[2-loop bubble]} + \text{[2-loop tadpole]} + \text{[2-loop bubble]} + \text{[2-loop tadpole]} \\
&+ \frac{i}{3} \frac{\zeta_\eta \zeta_\gamma^2}{f^4 \delta t^2} + \frac{i}{2} \frac{\zeta_\eta \zeta_\gamma^2}{f^4 \delta t^2} + \frac{i}{2} \frac{\zeta_\eta \zeta_\gamma^2}{f^4 \delta t^2} + \frac{i}{2} \frac{\zeta_\eta \zeta_\gamma^2}{f^4 \delta t^2} \\
&+ \text{[2-loop bubble]} + \text{[2-loop tadpole]} \\
&+ \frac{i}{2} \frac{\zeta_\eta \zeta_\gamma^2}{f^4 \delta t^2} + \frac{i}{4} \frac{\zeta_\eta \zeta_\gamma^2}{f^4 \delta t^2}
\end{aligned}$$

FIG. 10: Loop correction to $q_d^3 \dot{q}$ vertex in SK path integral (7). The sixth 2-loop diagram contains two topologically distinct diagrams which have reflection symmetry, as done in figure 9.

The propagators are obtained by taking functional derivative of \mathcal{Z}_0 w.r.t. the sources. The SK propagators are accordingly given by

$$\langle \dot{q}(t_2) \dot{q}(t_1) \rangle = (-1)^2 \frac{\partial^2 Z_0}{\partial J_q(t_2) \partial J_d(t_1)} \Big|_{J_{\dot{q}}, J_d, J_c, J_{\bar{c}}=0} = \int \frac{d\omega}{2\pi} \frac{f^r e^{-i\omega(t_2-t_1)}}{\omega^2 + (\gamma^r)^2}, \quad (\text{B10})$$

$$\langle q_d(t_2) \dot{q}(t_1) \rangle = (-1)^2 \frac{\partial^2 Z_0}{\partial J_{\dot{q}}(t_2) \partial J_d(t_1)} \Big|_{J_{\dot{q}}, J_d, J_c, J_{\bar{c}}=0} = - \int \frac{d\omega}{2\pi} \frac{e^{-i\omega(t_2-t_1)}}{\omega - i\gamma^r}, \quad (\text{B11})$$

$$\langle \dot{q}(t_2) q_d(t_1) \rangle = (-1)^2 \frac{\partial^2 Z_0}{\partial J_d(t_2) \partial J_{\dot{q}}(t_1)} \Big|_{J_{\dot{q}}, J_d, J_c, J_{\bar{c}}=0} = \int \frac{d\omega}{2\pi} \frac{e^{-i\omega(t_2-t_1)}}{\omega + i\gamma^r}, \quad (\text{B12})$$

$$\langle q_d(t_2) q_d(t_1) \rangle = (-1)^2 \frac{\partial^2 Z_0}{\partial J_{\dot{q}}(t_2) \partial J_{\dot{q}}(t_1)} \Big|_{J_{\dot{q}}, J_d, J_c, J_{\bar{c}}=0} = 0. \quad (\text{B13})$$

The first three propagators are called the Keldysh, advanced and retarded propagator respectively. Performing the ω integral we get

$$\langle \dot{q}(t_2) \dot{q}(t_1) \rangle = \frac{f^r}{2\gamma^r} e^{-\gamma^r |t_2-t_1|}, \quad (\text{B14})$$

$$\langle q_d(t_2) \dot{q}(t_1) \rangle = -i \Theta(t_1 - t_2) e^{-\gamma^r (t_1-t_2)}, \quad (\text{B15})$$

$$\langle \dot{q}(t_2) q_d(t_1) \rangle = -i \Theta(t_2 - t_1) e^{-\gamma^r (t_2-t_1)}, \quad (\text{B16})$$

$$\langle q_d(t_2) q_d(t_1) \rangle = 0. \quad (\text{B17})$$

We implement the above propagators in computation of real time correlation function in §III B and in §IV. Similarly the Grassmannian propagators are obtained as the following.

$$\begin{aligned} \langle \bar{c}(t_2) c(t_1) \rangle &= (-1)^2 \frac{\partial^2 Z_0}{\partial J_{\bar{c}}(t_2) \partial J_c(t_1)} \Big|_{J_{\dot{q}}, J_d, J_c, J_{\bar{c}}=0} \\ &= - \int \frac{d\omega}{2\pi} \frac{e^{-i\omega(t_2-t_1)}}{\omega - i\gamma}. \end{aligned} \quad (\text{B18})$$

Sub-leading correction to f^r, ζ_η^r due to $\bar{c}c$ loop:

The correction to f^r is obtained from a Grassmannian loop integral given by

$$\begin{aligned} (f^r)' &= f^r + (-1)(2i\zeta_\gamma)(-1) \int \frac{d\omega}{2\pi} \frac{1}{\omega - i\gamma} \\ &= f^r - \zeta_\gamma. \end{aligned} \quad (\text{B19})$$

The first (-1) appears due to the Grassmann loop, the factor $(2i\gamma)$ is the Feynman rules obtained from the effective path-integral (8). In our case $f^r = 5.29$ and $\zeta_\gamma = 0.0042$. So, the correction is smaller than the second order noise loop correction, thus can be ignored.

In a similar way we obtain the correction to ζ_γ^r , given by

$$\begin{aligned} (\zeta_\eta^r)' &= \zeta_\eta^r + (-1)(2i\zeta_\gamma)^2 \int \frac{d\omega}{2\pi} \frac{-1}{(\omega - i\gamma)(\omega + i\gamma)} \\ &= \zeta_\eta^r - \frac{2\zeta_\gamma^2}{\gamma}. \end{aligned} \quad (\text{B20})$$

The correction is again sufficiently small. Thus we conclude that the Grassmannian correction, for the domain of our parameters, does not significantly contribute to correlation function.

-
- [1] B. Chakrabarty and S. Chaudhuri, Out of time ordered effective dynamics of a quartic oscillator, *SciPost Phys.* **7**, 013 (2019), [arXiv:1905.08307 \[hep-th\]](#).
 - [2] B. Chakrabarty, S. Chaudhuri, and R. Loganayagam, Out of Time Ordered Quantum Dissipation, *JHEP* **07**, 102, [arXiv:1811.01513 \[cond-mat.stat-mech\]](#).
 - [3] B. Chakrabarty, J. Chakravarty, S. Chaudhuri, C. Jana, R. Loganayagam, and A. Sivakumar, Nonlinear Langevin dynamics via holography, *JHEP* **01**, 165, [arXiv:1906.07762 \[hep-th\]](#).
 - [4] C. Jana, R. Loganayagam, and M. Rangamani, Open quantum systems and Schwinger-Keldysh holograms, *JHEP* **07**, 242, [arXiv:2004.02888 \[hep-th\]](#).
 - [5] J. S. Schwinger, Brownian motion of a quantum oscillator, *J. Math. Phys.* **2**, 407 (1961).
 - [6] L. V. Keldysh, Diagram technique for nonequilibrium processes, *Zh. Eksp. Teor. Fiz.* **47**, 1515 (1964), [Sov. Phys. JETP **20**, 1018 (1965)].
 - [7] E. Calzetta and B. L. Hu, Closed Time Path Functional Formalism in Curved Space-Time: Application to Cosmological Back Reaction Problems, *Phys. Rev.* **D35**, 495 (1987).
 - [8] A. Kamenev, *Field Theory of Non-Equilibrium Systems* (Cambridge University Press, Cambridge, 1985).
 - [9] P. C. Martin, E. D. Siggia, and H. A. Rose, Statistical Dynamics of Classical Systems, *Phys. Rev. A* **8**, 423 (1973).
 - [10] C. De Dominicis and L. Peliti, Field Theory Renormalization and Critical Dynamics Above $t(c)$: Helium, Antiferromagnets and Liquid Gas Systems, *Phys. Rev. B* **18**, 353 (1978).
 - [11] H. Janssen, On a lagrangean for classical field dynamics and renormalization group calculations of dynamical critical properties, *Zeitschrift für Physik B Condensed*

- Matter and Quanta **23**, 377 (1976).
- [12] J. Berges and J. Cox, Thermalization of quantum fields from time reversal invariant evolution equations, *Phys. Lett. B* **517**, 369 (2001), [arXiv:hep-ph/0006160](#).
 - [13] C. Maes and K. Netocny, Time-Reversal and Entropy, *arXiv e-prints*, cond-mat/0202501 (2002), [arXiv:cond-mat/0202501 \[cond-mat.stat-mech\]](#).
 - [14] R. J. Harris and G. M. Schütz, Fluctuation theorems for stochastic dynamics, *Journal of Statistical Mechanics: Theory and Experiment* **2007**, P07020 (2007).
 - [15] J. M. R. Parrondo, C. V. den Broeck, and R. Kawai, Entropy production and the arrow of time, *New Journal of Physics* **11**, 073008 (2009).
 - [16] D. Andrieux, P. Gaspard, T. Monnai, and S. Tasaki, The fluctuation theorem for currents in open quantum systems, *New Journal of Physics* **11**, 043014 (2009).
 - [17] E. H. Feng and G. E. Crooks, Length of time's arrow, *Phys. Rev. Lett.* **101**, 090602 (2008).
 - [18] J. von Neumann, Various techniques used in connection with random digits, in *Monte Carlo Method*, National Bureau of Standards Applied Mathematics Series, Vol. 12, edited by A. S. Householder, G. E. Forsythe, and H. H. Germond (US Government Printing Office, Washington, DC, 1951) Chap. 13, pp. 36–38.
 - [19] I. Oppenheim, Nonlinear nonequilibrium thermodynamics i. linear and nonlinear fluctuation-dissipation theorems, *Journal of Statistical Physics* **77**, 1109 (1994).
 - [20] R. L. Stratonovich, Nonlinear nonequilibrium thermodynamics ii (1992).
 - [21] S. Chaudhuri, Unpublished notes, .
 - [22] S. Chib and E. Greenberg, Understanding the metropolis-hastings algorithm, *The American Statistician* **49**, 327 (1995), <https://www.tandfonline.com/doi/pdf/10.1080/00031305.1995.10476>.
 - [23] R. P. Feynman and F. L. Vernon, Jr., The Theory of a general quantum system interacting with a linear dissipative system, *Annals Phys.* **24**, 118 (1963), [*Annals Phys.*281,547(2000)].
 - [24] L. Onsager, Reciprocal Relations in Irreversible Processes. I., *Phys. Rev.* **37**, 405 (1931).
 - [25] L. Onsager, Reciprocal Relations in Irreversible Processes. II., *Phys. Rev.* **38**, 2265 (1931).
 - [26] H. B. G. Casimir, On onsager's principle of microscopic reversibility, *Rev. Mod. Phys.* **17**, 343 (1945).
 - [27] F. Haehl, R. Loganayagam, and M. Rangamani, Schwinger-keldysh formalism i: Brst symmetries and superspace, *Journal of High Energy Physics* **2017** (2016).
 - [28] F. M. Haehl, R. Loganayagam, P. Narayan, and M. Rangamani, Classification of out-of-time-order correlators, *SciPost Phys.* **6**, 001 (2019), [arXiv:1701.02820 \[hep-th\]](#).
 - [29] S. Chaudhuri, C. Chowdhury, and R. Loganayagam, Spectral Representation of Thermal OTO Correlators, *JHEP* **02**, 018, [arXiv:1810.03118 \[hep-th\]](#).
 - [30] S. Chaudhuri and R. Loganayagam, Probing Out-of-Time-Order Correlators, *JHEP* **07**, 006, [arXiv:1807.09731 \[hep-th\]](#).